Molecular and Cellular Endocrinology 479 (2019) 117–122

Contents lists available at ScienceDirect

Molecular and Cellular Endocrinology

journal homepage: www.elsevier.com/locate/mce

Androgen receptor SUMOylation regulates bone mass in male mice

Jianyao Wu[a], Sofia Movérare-Skrtic[a], Fu-Ping Zhang[b], Antti Koskela[c], Juha Tuukkanen[c], Jorma J. Palvimo[d], Petra Sipilä[b], Matti Poutanen[a,b,1], Claes Ohlsson[a,*,1]

[a] Centre for Bone and Arthritis Research, Institute of Medicine, Sahlgrenska Academy, University of Gothenburg, Gothenburg, Sweden
[b] Institute of Biomedicine and Turku Center for Disease Modeling, University of Turku, Turku, Finland
[c] Department of Anatomy and Cell Biology, Medical Research Center, University of Oulu, Oulu, Finland
[d] Institute of Biomedicine, University of Eastern Finland, Kuopio, Finland

ARTICLE INFO

Keywords:
Androgen receptor
SUMOylation
Posttranslational modification
Bone

ABSTRACT

The crucial effects of androgens on the male skeleton are at least partly mediated via the androgen receptor (AR). In addition to hormone binding, the AR activity is regulated by post-translational modifications, including SUMOylation. SUMOylation is a reversible modification in which Small Ubiquitin-related MOdifier proteins (SUMOs) are attached to the AR and thereby regulate the activity of the AR and change its interactions with other proteins.

To elucidate the importance of SUMOylation of AR for male bone metabolism, we used a mouse model devoid of the two AR SUMOylation sites (AR^{SUM-}; K381R and K500R are substituted). Six-month-old male AR^{SUM-} mice displayed significantly reduced trabecular bone volume fraction in the distal metaphyseal region of femur compared with wild type (WT) mice (BV/TV, $-19.1 \pm 4.9\%$, $P < 0.05$). The number of osteoblasts per bone perimeter was substantially reduced ($-60.5 \pm 7.2\%$, $P < 0.001$) while no significant effect was observed on the number of osteoclasts in the trabecular bone of male AR^{SUM-} mice. Dynamic histomorphometric analysis of trabecular bone revealed a reduced bone formation rate ($-32.6 \pm 7.4\%$, $P < 0.05$) as a result of reduced mineralizing surface per bone surface in AR^{SUM-} mice compared with WT mice ($-24.3 \pm 3.6\%$, $P < 0.001$). Furthermore, cortical bone thickness in the diaphyseal region of femur was reduced in male AR^{SUM-} mice compared with WT mice ($-7.3 \pm 2.0\%$, $P < 0.05$).

In conclusion, mice devoid of AR SUMOylation have reduced trabecular bone mass as a result of reduced bone formation. We propose that therapies enhancing AR SUMOylation might result in bone-specific anabolic effects with minimal adverse effects in other tissues.

1. Introduction

The crucial role of androgens for male bone health is well documented (Callewaert et al., 2009; Falahati-Nini et al., 2000; Kawano et al., 2003; Leder et al., 2003; Orwoll, 2001; Vanderschueren et al., 2014). Although a substantial part of the effects of androgens on the skeleton is mediated via conversion of testosterone to estradiol, direct effects of androgens on the androgen receptor (AR) clearly contribute to male bone homeostasis (Almeida et al., 2017; Khosla and Monroe, 2017; Mellström et al., 2008; Vanderschueren et al., 2014). This notion is supported by that male mice with global deletion of the AR have reduced trabecular and cortical bone mass (Callewaert et al., 2009; Kawano et al., 2003). Studies using cell specific gene deletions of the AR have demonstrated that AR expressed in osteoblast lineage cells mediates the protective effects of androgens on trabecular bone mass, while the target cell(s) of the actions of androgens on cortical bone mass remains unknown (Almeida et al., 2017; Vanderschueren et al., 2014).

The AR activity can be regulated by several different post-translational modifications (PTMs), including phosphorylation, acetylation, SUMOylation, ubiquitination and methylation (Coffey and Robson, 2012). The importance of PTMs in the AR for male bone metabolism is unknown. SUMOylation is a reversible modification in which Small Ubiquitin-related MOdifier proteins are covalently attached to the target proteins' specific lysine residue and thereby it regulates diverse cellular processes, including transcription, replication, chromosome segregation, and DNA repair (Gareau and Lima, 2010; Wilkinson and Henley, 2010). Substrate modification by SUMOylation can alter

* Corresponding author. Centre for Bone and Arthritis Research, Vita Stråket 11, Sahlgrenska University Hospital, S-413 45, Gothenburg, Sweden.
E-mail address: claes.ohlsson@medic.gu.se (C. Ohlsson).
[1] Contributed equally.

https://doi.org/10.1016/j.mce.2018.09.008
Received 27 April 2018; Received in revised form 22 September 2018; Accepted 22 September 2018
Available online 24 September 2018
0303-7207/ © 2018 The Authors. Published by Elsevier B.V. This is an open access article under the CC BY-NC-ND license (http://creativecommons.org/licenses/BY-NC-ND/4.0/).

protein-protein interactions, change the intracellular localization of the protein, or in few cases, directly change the activity of the protein to which SUMO is attached (Coffey and Robson, 2012). There are three members of the SUMO protein family that can be conjugated to proteins: SUMO1, SUMO2 and SUMO3. SUMO2 and SUMO3 differ from each other by only three N-terminal residues and are often referred to collectively as SUMO2/3. In contrast, SUMO2/3 share only 50% similarity with SUMO1 (Wilkinson and Henley, 2010). AR SUMOylation is a reversible process achieved by a family of SUMO proteases termed Sentrin/SUMO-specific proteases (SENPs) (Poukka et al., 2000).

In humans, AR SUMOylation occurs within the N-terminal domain of the protein at Lys386 (Lys381 in mouse) and Lys520 (Lys500 in mouse). *In vitro* experiments established that reversible SUMOylation is a mechanism for regulation of AR function (Poukka et al., 2000). The initial *in vitro* studies indicated that AR SUMOylation mainly reduced AR activity, while a subsequent more detailed functional *in vitro* study revealed that AR SUMOylation also lead to increased AR-dependent transcription (Kaikkonen et al., 2009; Poukka et al., 2000; Sutinen et al., 2014). In the later study, the role of the two AR SUMOylation sites was evaluated by comparing cell lines expressing WT AR with cell lines expressing doubly SUMOylation site-mutated AR (Sutinen et al., 2014). Genome-wide gene expression analyses of these cell lines revealed that AR SUMOylation modulates the AR function in a target gene and pathway selective manner. Besides, SUMOylation mutant AR cells actually proliferated faster than the WT cells. These data indicate that AR SUMOylation does not simply repress the AR activity, but regulates AR's interaction with the chromatin and the receptor's target gene selection and that this might occur in a promoter specific and cell-type specific context (Sutinen et al., 2014).

Based on these finding, we hypothesized that AR SUMOylation might result in tissue specific effects *in vivo* in male mice and that increased knowledge of the possible tissue specificity of the role of AR SUMOylation may result in the development of bone-specific anabolic treatments with minimal adverse effects in other androgen responsive tissues. Although AR SUMOylation is extensively studied *in vitro* mainly using prostate cancer cells, the physiological role of AR SUMOylation *in vivo* in mice is unknown (Kaikkonen et al., 2009; Poukka et al., 2000; Sutinen et al., 2014). To elucidate the importance of AR SUMOylation for male bone metabolism, we used a mouse model devoid of the two AR SUMOylation sites (AR^{SUM-}; K381R and K500R are substituted).

2. Materials and methods

2.1. Description of a mouse model devoid of AR SUMOylation sites

We used a genetically engineered mouse knock-in model devoid of AR SUMOylation at the two lysine residues at the exon 1. In the mutant mice these two conserved lysine residues were replaced by arginine residues (K381R and K500R) using site-directed mutagenesis to permanently abolish the SUMO attachment (Fig. 1A). The targeting construct was verified by sequencing. The mice were generated using standard techniques by applying homologous recombination in the mouse ES cells, using a fragment containing exon 1 with the mutations and a Neo cassette. The Neo cassette was then removed *in vitro*, and mutated mice were generated via routine techniques using blastocyst injection. After establishing the mouse line the genotypes of the mice were verified by PCR on ear biopsies. The female mice heterozygous for the targeted allele on the X-chromosome were crossed to male C57BL/6J wild type (WT) mice resulting in 50% WT males (=control male siblings) and 50% males with the mutated allele (AR^{SUM-}). Further description of the generation of the mouse model used is presented elsewhere and part of the data in this article has been presented at the ASBMR Annual meeting in 2016 (Wu, et al., 2016).

At six months of age, the blood was collected from the heart under anesthesia, and the mice were subsequently sacrificed by cervical dislocation. Bones were collected and fixed in 4% formalin or stored in −20 °C until analyses. All the animal experimental procedures were approved by the ethics committee of University of Turku, Finland.

2.2. High-resolution micro-computed tomography (μCT)

High-resolution μCT analyses were performed on the distal femur using an 1172 model micro-CT (Bruker micro-CT, Aartselaar, Belgium) (Moverare-Skrtic et al., 2014). The femur were imaged with an X-ray tube voltage of 50 kV and a current of 200 μA, with a 0.5-mm aluminium filter. The scanning angular rotation was 180°, and the angular increment was 0.70°. The voxel size was 4.49 μm isotropically. NRecon (version 1.6.9) was employed to perform the reconstruction after scans. Trabecular bone proximal to the distal growth plate in femur was selected for analyses within a conforming volume of interest (cortical bone excluded) commencing at a distance of 427 μm from the growth plate and extending a further longitudinal 135 μm in the proximal direction. Cortical measurements were performed in the diaphyseal region of the femur starting at a distance of 5.2 mm from the growth plate and extending a further longitudinal 135 μm in the proximal direction. For BMD analysis, the equipment was calibrated with ceramic standard samples (Bruker, Aartselaar, Belgium).

2.3. Histomorphometric analyses

The mice were double labeled with calcein (i.p. 50 mg/kg, Sigma-aldrich Sweden AB, Stockholm, Sweden) and alizarin (i.p. 50 mg/kg, Sigma-aldrich Sweden AB, Stockholm, Sweden) 8 days and 1 day before termination, respectively. Bone histomorphometry was performed on the distal metaphyseal trabecular bone and the mid-diaphyseal cortical bone in femur (Erben and Glosmann, 2012). Each femur was dissected into two regions, one including distal epiphysis and metaphysis and one including femoral shaft. Both femoral regions were embedded in methyl methacrylate.

The distal epiphysis and metaphysis of femur was sectioned longitudinally using a fully motorized rotary microtome and a tungsten-carbide knife. Plastic sections were obtained from a standardized site of metaphyseal marrow cavity. Static parameters were determined in a 4-μm-thick section stained in Masson-Goldner's Trichrome and dynamic parameters in an unstained 8-μm-thick section.

Each embedded femoral shaft was sectioned in a transverse plane using a linear precision saw and a diamond blade. A plastic section with the thickness of 200 μm was obtained from a standardized site of femoral shaft. The analyses of static and dynamic parameters were performed in diaphyseal cortical bone without any staining.

All parameters were analyzed using OsteoMeasure histomorphometry system (OsteoMetrics, Atlanta, GA, USA), following the guidelines of the American Society for Bone and Mineral Research (Dempster et al., 2013).

2.4. Biomechanical strength analyses

Tibia was loaded by three-point bending test (span length 5.5 mm) (Wu et al., 2016). Loading speed for tibia was 0.155 mm/s with a mechanical testing machine (Instron 3366, Instron, Norwood, MA, USA). Based on the computer recorded load deformation raw data curves, produced by Bluehill 2 software v2.6 (Instron), the results were calculated with custom-made Excel macros.

2.5. Serum analyses

Blood samples were allowed to clot and were then centrifuged (10000 × g, 10 min, 4 °C). Serum levels of testosterone were measured in a single run by GC-MS/MS (Nilsson et al., 2015). After the addition of isotope-labeled standards, steroids were extracted to chlorobutane, purified on a silica column and derivatized using pentafluorobenzylhydroxylamine hydrochloride followed by

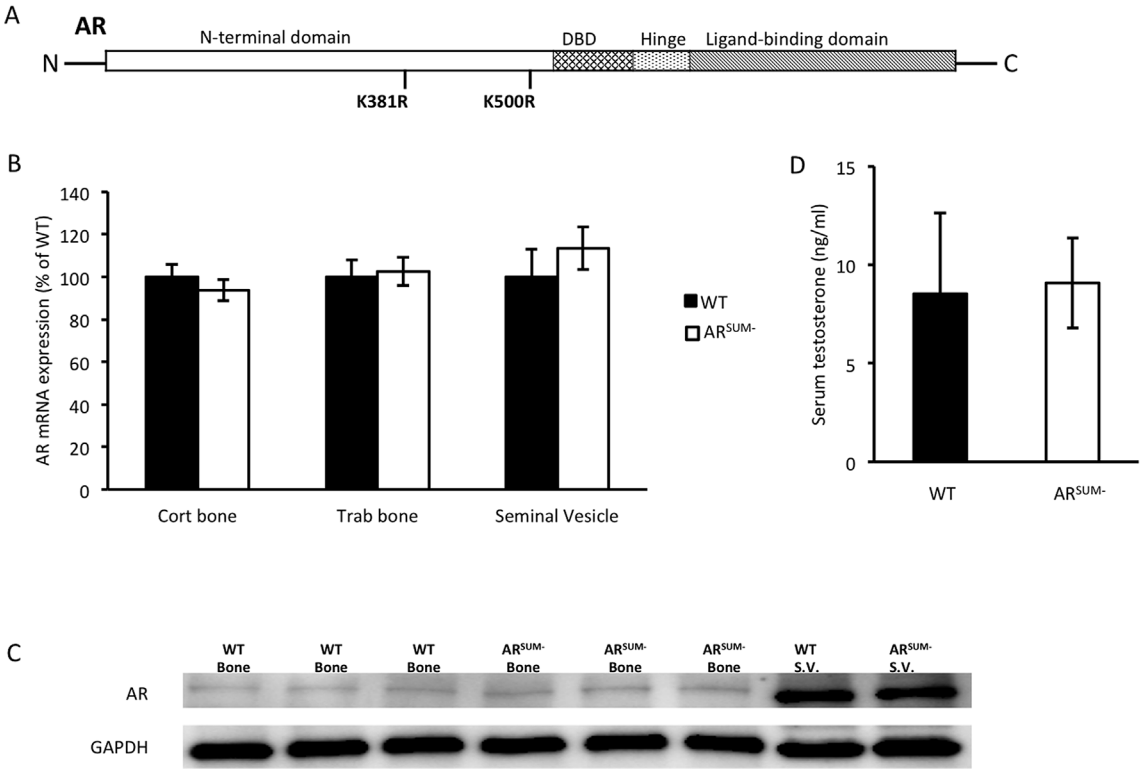

Fig. 1. Description of a mouse model devoid of androgen receptor (AR) SUMOylation sites
(A) Schematic presentation of the AR in the AR^{SUM-} mouse model with lysine-to-arginine mutations at positions 381 and 500 in the N-terminal domain of AR. (B) AR mRNA levels in cortical bone (Cort), trabecular bone (Trab), and seminal vesicle of six-month-old male AR^{SUM-} and wild type (WT) mice, expressed as percent of expression in WT mice. (C) Western blot analysis of AR protein levels in bone and seminal vesicle (S.V.) of six-month-old male AR^{SUM-} and WT mice. The lanes present samples from individual mice. (D) Serum testosterone levels as measured by GC-MS/MS in six-month-old male AR^{SUM-} and WT mice. DBD: DNA-binding domain. Values are given as mean ± sem. [n = 10–16].

pentafluorobenzoyl chloride. Testosterone was analyzed in multiple reactions monitoring mode with ammonia as reagent gas using an Agilent 7000 triple quadrupole mass spectrometer equipped with a chemical ionization source. Serum levels of C-terminal type I collagen (CTX) fragments were assessed using an ELISA RatLaps kit (Immunodiagnostic Systems, Tyne and Wear, UK) according to the manufacturer's instructions. Serum levels of osteocalcin (OCN) were determined with a mouse osteocalcin immunosorbent assay kit (Immutopics, Athens, USA).

2.6. Quantitative real-time PCR analysis

Total RNA was prepared from mid-diaphyseal cortical bone of the tibia and vertebral body of vertebrae L_6 (trabecular bone), using TRIzol reagent (Life Technologies) followed by the RNeasy Mini Kit (Qiagen). The RNA was reverse transcribed into cDNA, and real-time PCR analysis was performed using predesigned real-time PCR assay for AR (Mm00442688_m1) on the StepOnePlus Real-Time PCR system (Applied Biosystems). The mRNA abundance of AR was adjusted for the expression of 18S.

2.7. Western blotting

Western blot analysis of seminal vesicle and bone from WT and AR^{SUM-} mice were adapted from the methods as previously described (Gustafsson et al., 2016). Tissues were homogenized in NP-40 cell lysis buffer supplemented with complete Mini EDTA-free Protease Inhibitor Cocktail (Roche Diagnostics), and incubated on ice for 1 h. Following centrifugation at 12000 × g for 10 min at 4 °C, the supernatant was collected. Extracted proteins concentrations were further determined using Bovine Serum Albumin (BSA) as standard by bicinchoninic acid protein assay (Pierce, Rockford, IL, USA). Equal amount of each sample was loaded and run on AnykD Mini-PROTEAN TGX Precast Protein Gels (Bio-Rad) at 200 V and transferred to Immun-Blot Low Fluorescence PVDF Membranes using Trans-Blot Turbo Transfer System (Bio-Rad). Membranes were blocked in 5% milk for 1 h at room temperature and incubated overnight with rabbit polyclonal anti-AR (C-19) (dilution 1:100; Santa Cruz Biotechnology) or GADPH antibody (dilution 1:5000). Secondary incubation by TidyBlot dectection reagent (1:500, Bio-Rad) and Clarity Max Western ECL substrate (Bio-Rad) were used to visualize the bands.

2.8. Statistical analyses

Values are given as mean ± sem. The statistical differences between WT and AR^{SUM-} mice were calculated using Student's *t*-test.

3. Results

3.1. Description of a mouse model devoid of AR SUMOylation sites

We used a mouse model devoid of the two AR SUMOylation sites (AR^{SUM-}; K381R and K500R are substituted; Fig. 1A). Six-month-old AR^{SUM-} mice were apparently healthy and had normal AR mRNA and protein levels in both seminal vesicles and bone, demonstrating that the targeting strategy did not influence AR expression (Fig. 1B and C). In addition, the serum levels of testosterone were not affected in the AR^{SUM-} mice (Fig. 1D), strongly suggesting that AR^{SUM-} mice do not have a disturbed feedback regulation of serum androgen levels.

Table 1
Body characteristics.

	WT	AR^{SUM-}
Body weight (g)	34.9 ± 1.0	37.3 ± 1.1
Tibia length (mm)	19.2 ± 0.1	19.3 ± 0.1
Femur length (mm)	16.4 ± 0.1	16.6 ± 0.1
Organ weight/Body weight		
Prostate (%)	0.036 ± 0.004	0.027 ± 0.004
Seminal vesicle (%)	1.16 ± 0.08	1.06 ± 0.08
Musculus levator ani (%)	0.29 ± 0.01	0.31 ± 0.01

Body characteristics of six-month-old male AR^{SUM-} and wild type (WT) mice. Values are given as mean ± sem. [n = 10–16].

3.2. Male mice devoid of AR SUMOylation display normal weights of well-established androgen responsive tissues

AR^{SUM-} mice displayed no change in body weight or bone lengths compared with WT mice (Table 1). We next evaluated the phenotype of some major (non-bone) androgen responsive tissues in AR^{SUM-} mice. The weights of prostate, seminal vesicles, and musculus levator ani were unchanged in the AR^{SUM-} mice, strongly suggesting that there was no major overall alteration in AR sensitivity in the AR^{SUM-} mice (Table 1).

3.3. Male mice devoid of AR SUMOylation display reduced trabecular and cortical bone mass

Trabecular bone volume fraction (BV/TV) in the distal metaphyseal region of femur was significantly lower in AR^{SUM-} mice as compared with WT mice (−19.1 ± 4.9%, $P < 0.05$; Fig. 2A) and this was associated with an increased trabecular separation (+20.1 ± 3.7%, $P < 0.01$; Table 2). Analysis of the cortical bone compartment using μCT demonstrated decreased cortical area (−12.1 ± 2.2%, $P < 0.001$; Fig. 2B) and cortical thickness (−7.3 ± 2.0%, $P < 0.05$; Fig. 2C) of femur in adult AR^{SUM-} male mice compared with WT mice. The decreased cortical thickness was mainly due to decreased periosteal circumferences (−5.6 ± 1.6%, $P < 0.05$; Table 2). A reduced periosteal circumference was supported by that the total bone area was decreased by 11.9% ($P < 0.001$) in femur of AR^{SUM-} mice compared with WT mice when evaluated using static histomorphometry (Table 2). Neither cortical volumetric density nor cortical porosity was affected in the AR^{SUM-} male mice compared with WT mice (Table 2). Three-point bending analyses of the tibia diaphysis revealed that the stiffness but not the maximal load was significantly reduced in the AR^{SUM-} mice compared with WT mice (Table 2).

Table 2
Bone parameters.

	WT	AR^{SUM-}
Trabecular bone, μCT femur		
Separation (Tb.Sp; μm)	86.5 ± 2.8	103.9 ± 3.2***
Number (Tb.N; mm^{-1})	3.9 ± 0.2	3.3 ± 0.2
Thickness (Tb.Th; μm)	49.6 ± 1.5	46.5 ± 0.9
Cortical bone, μCT femur		
Periosteal circumference (mm)	6.5 ± 0.1	6.1 ± 0.1*
Endocortical circumference (mm)	5.5 ± 0.1	5.2 ± 0.1
Cortical volumetric density (mg/mm^3)	1.28 ± 0.01	1.28 ± 0.01
Cortical porosity (%)	1.82 ± 0.13	1.76 ± 0.11
Cortical bone, histomorphometry femur		
Total bone area (B.Ar; mm^2)	2.53 ± 0.05	2.23 ± 0.05***
Marrow cavity area (Ma. Ar; mm^2)	1.36 ± 0.06	1.20 ± 0.04*
Cortical bone area (Ct.Ar; mm^2)	1.17 ± 0.03	1.03 ± 0.03*
Periosteal bone formation rate/bone surface ($\mu m^3/\mu m^2/y$)	156 ± 29	134 ± 20
Endocortical bone formation rate/bone surface ($\mu m^3/\mu m^2/y$)	248 ± 23	222 ± 23
Mechanical test, three point bending tibia		
Fmax (N)	22.5 ± 1.5	23.7 ± 1.0
Stiffness (N/mm)	180 ± 7	158 ± 5*
Serum bone markers		
CTX (ng/ml)	49.2 ± 5.1	46.0 ± 2.5
OCN (ng/ml)	25.9 ± 1.6	25.1 ± 1.3

Bone parameters in six-month-old AR^{SUM-} and wild type (WT) mice. Values are given as mean ± sem. [n = 10–16]. *$P < 0.05$, ***$P < 0.001$. AR^{SUM-} vs. WT. Student's *t*-test vs. WT.
CTX = C-terminal type I collagen fragments, OCN = osteocalcin.

3.4. Male mice devoid of AR SUMOylation display reduced bone formation

Static and dynamic histomorphometry was used to determine the mechanism for the reduced bone mass in male AR^{SUM-} mice. Static histomorphometry revealed that the number of osteoblasts per bone perimeter was substantially reduced (−60.5 ± 7.2%, $P < 0.001$) while no significant effect was observed on the number of osteoclasts or osteocytes in the trabecular bone of male AR^{SUM-} mice compared with WT mice (Fig. 3A–C). Dynamic histomorphometric analysis demonstrated reduced trabecular bone formation rate (BFR; −32.6 ± 7.4%, $P < 0.05$) in AR^{SUM-} mice compared with WT mice (Fig. 3D). The decreased BFR in the AR^{SUM-} mice was mainly due to decreased mineralizing surface per bone surface (MS/BS; −24.3 ± 3.6%, $P < 0.001$), whereas the mineral apposition rate (MAR) was unaffected (Fig. 3E–F). Dynamic histomorphometry of the diaphyseal cortical bone in femur did not identify any significant difference in periosteal or endosteal BFR in six-month-old male AR^{SUM-} mice

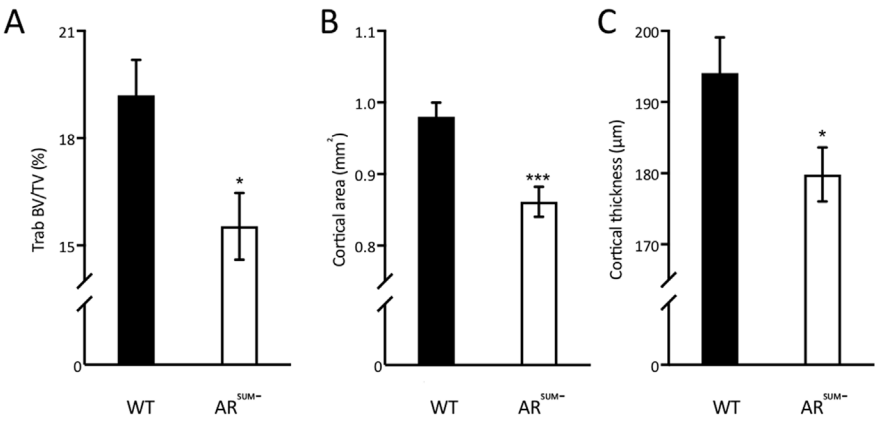

Fig. 2. Male mice devoid of androgen receptor (AR) SUMOylation display reduced trabecular and cortical bone mass
(A) Trabecular (Trab) bone volume per tissue volume (BV/TV), (B) cortical area, and (C) cortical thickness as analyzed by μCT in the femur of six-month-old male AR^{SUM-} and wild type (WT) mice. Values are given as mean ± sem. [n = 10–16]. *$P < 0.05$ and ***$P < 0.001$ Student's *t*-test vs. WT.

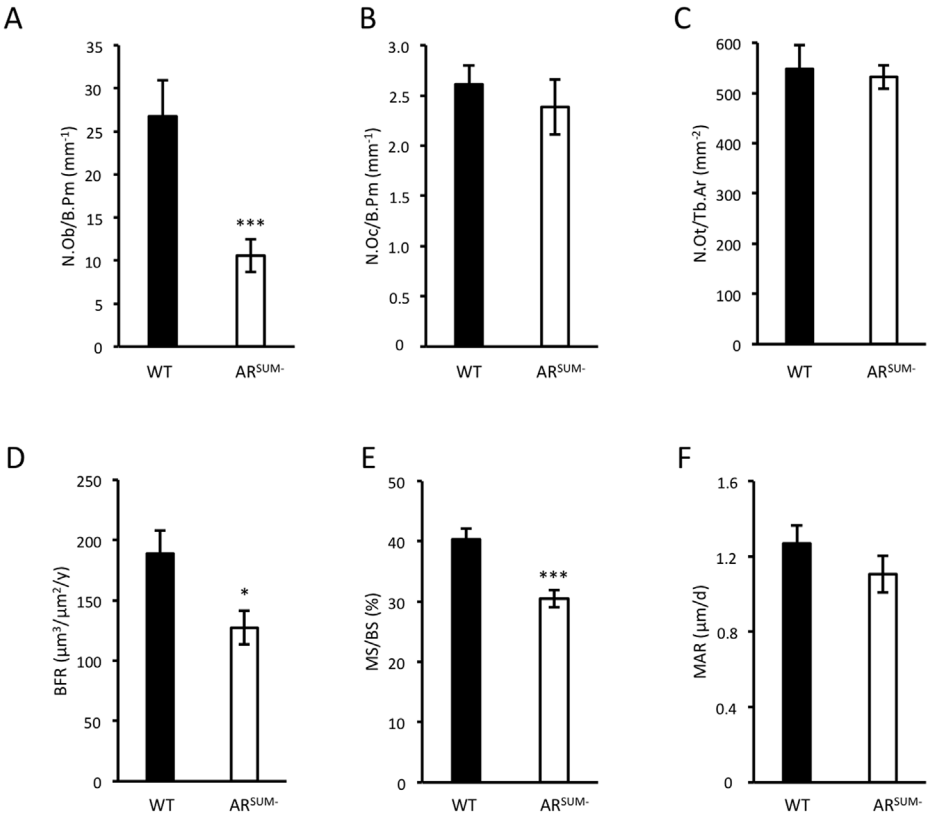

Fig. 3. Male mice devoid of androgen receptor (AR) SUMOylation display reduced bone formation (A) Number of osteoblast per bone perimeter (N.Ob/B.Pm), (B) number of osteoclast per bone perimeter (N.Oc/B.Pm), (C) number of osteocytes per trabecular area (N.Ot/Tb.Ar), (D) bone formation rate (BFR), (E) mineral surface per bone surface (MS/BS), and (F) mineral apposition rate (MAR) as analyzed by histomorphometry in femur of six-month-old male AR^{SUM-} and wild type (WT) mice. Values are given as mean ± sem. [n = 10–16]. *P < 0.05 and ***P < 0.001 Student's *t*-test vs. WT.

compared with WT mice (Table 2). Neither serum levels of C-terminal type I collagen fragments (CTX) nor serum levels of osteocalcin were significantly affected in the AR^{SUM-} mice compared with WT mice (Table 2).

4. Discussion

Although it is well-established that the AR is required for normal bone metabolism in male mice, the role of PTMs in the AR for male bone metabolism is unknown (Callewaert et al., 2009; Kawano et al., 2003; Vanderschueren et al., 2014). SUMOylation is a PTM with substantial effects on AR activity *in vitro* but its role for tissue-specific AR activity *in vivo* is unknown (Kaikkonen et al., 2009; Poukka et al., 2000; Sutinen et al., 2014). We, herein, demonstrate that male mice devoid of AR SUMOylation had reduced bone mass while the weights of several well-established androgen responsive tissues were unchanged, suggesting that the *in vivo* effects of AR SUMOylation are tissue specific with a clear effect in bone.

The number of studies evaluating the effects of PTMs in nuclear receptors for bone metabolism is limited, but we recently demonstrated that palmitoylation of estrogen receptor-α is required for the estrogenic response in bone (Gustafsson et al., 2016; Vinel et al., 2016). There is no previous study evaluating the bone metabolism in mice with PTMs in the AR. However, the effect of SUMOylation of AR has been thoroughly characterized *in vitro* mainly using prostate cancer cells, revealing that SUMOylation has the capacity to regulate the activity of the AR (Sutinen et al., 2014). To evaluate the specific role of AR SUMOylation for bone mass, we generated a mouse model devoid of the two AR SUMOylation sites. The male AR^{SUM-} mice were apparently healthy, displayed a normal longitudinal bone growth, had normal AR levels in bone and seminal vesicles and had no signs of disturbed feed-back regulation of serum testosterone, demonstrating that it is a valid *in vivo* model to evaluate the tissue specific physiological effects of AR SUMOylation.

The main finding in the present study is that male AR^{SUM-} mice have reduced trabecular and cortical bone mass. Since mice with global AR inactivation also display reduced trabecular and cortical bone mass (Callewaert et al., 2009; Kawano et al., 2003; Vanderschueren et al., 2014), it is likely that AR SUMOylation results in enhanced AR activity in bone. This is in contrast to the early *in vitro* studies using prostate cancer cells suggesting that AR SUMOylation reduces AR activity but subsequent more thorough studies revealed that SUMOylation of AR also may increase AR mediated transcription in a promoter specific and cell-type specific context (Kaikkonen et al., 2009; Poukka et al., 2000; Sutinen et al., 2014). It is possible that different members of the SUMO protein family (SUMO1, SUMO2 and SUMO3) may affect AR mediated transcription differentially. Earlier *in vitro* studies of AR SUMOylation focused on the addition of SUMO1 to the AR, but later studies demonstrated that SUMO2 and SUMO3 also could function as AR regulators (Kaikkonen et al., 2009; Poukka et al., 2000; Sutinen et al., 2014). In contrast to SUMO1, which inhibits AR activity, SUMO2 and SUMO3 enhance the AR transcriptional activity in prostate cancer cells. The relative roles of the different SUMO proteins for the overall stimulatory effect of AR SUMOylation on bone mass remain to be determined.

In contrast to bone mass, the weights of well-established androgen responsive tissues including prostate, seminal vesicles and musculus levator ani were unchanged in male AR^{SUM-} mice. These findings demonstrate that the physiological role of AR SUMOylation *in vivo* is tissue-specific with a clear role for bone metabolism while some other major androgen dependent tissues are unaffected. We propose that therapies enhancing AR SUMOylation might result in bone-specific anabolic effects with minimal adverse effects in other tissues.

The stimulatory effect of androgens on trabecular bone mass is at least partly mediated via ARs on osteoblast lineage cells (Almeida et al., 2017). Male AR^{SUM-} mice displayed significantly reduced trabecular bone volume fraction as a result of increases trabecular separation. This was mainly caused by reduced bone formation supported by reduced number of osteoblasts while number of osteoclasts was unaffected in the trabecular bone of male AR^{SUM-} mice. A reduced bone formation

was also supported by dynamic histomorphometric analyses of trabecular bone, revealing reduced bone formation rate as a result of reduced mineralizing surface per bone surface in AR^{SUM-} mice compared with WT mice. Collectively, these findings demonstrate that AR SUMOylation results in activation of osteoblasts and thereby increased bone formation in trabecular bone.

It is well-established that androgens and the AR are required for cortical radial bone growth in male mice (Vanderschueren et al., 2014). The AR^{SUM-} mice had reduced cortical bone thickness as a result of reduced periosteal circumference, indicating that AR SUMOylation is required for normal radial bone growth in male mice. However, dynamic histomorphometry of the diaphyseal cortical bone in femur did not identify any significant difference in periosteal bone formation rate when evaluated in adult male AR^{SUM-} mice compared with WT mice, suggesting that AR SUMOylation is required for normal radial bone expansion during development and growth while it is dispensable for adult cortical bone metabolism. The observed unchanged serum osteocalcin in the adult AR^{SUM-} mice is most likely the result of the unchanged cortical bone formation rate.

In conclusion, mice devoid of AR SUMOylation have reduced trabecular bone mass as a result of reduced bone formation. We propose that therapies enhancing AR SUMOylation might result in bone-specific anabolic effects with minimal adverse effects in other tissues.

Authors contributions

Study design: CO, MP, JJP, PS, JW, SMS. Study conduct: FPZ. Data collection: JW, SMS, PS, JJP, FPZ. Data analysis: JW, SMS, AK, JT. Data interpretation: CO, SMS, JW, MP. Drafting manuscript: JW, SMS, CO. Statistical analysis: JW, CO, SMS.

Funding

Swedish Research Council.
Swedish Foundation for Strategic Research.
ALF/LUA research grant from the Sahlgrenska University Hospital.
Lundberg Foundation.
The European Calcified Tissue Society.
Torsten and Ragnar Söderberg's Foundation.
Novo Nordisk Foundation.
Knut and Alice Wallenberg Foundation.
Academy of Finland.

Disclosures

All authors state that they have no conflicts of interest.

Acknowledgements

This study is supported by the Swedish Research Council, the Swedish Foundation for Strategic Research, the ALF/LUA research grant from the Sahlgrenska University Hospital, the Lundberg Foundation, the European Calcified Tissue Society, the Torsten and Ragnar Söderberg's Foundation, Knut and Alice Wallenberg Foundation, the Academy of Finland and the Novo Nordisk Foundation. We are grateful to C. Uggla, A. Hansevi, B. Aleksic and the staff at the Turku Center for Disease Modeling (TCDM) for technical assistance.

References

Almeida, M., Laurent, M.R., Dubois, V., Claessens, F., O'Brien, C.A., Bouillon, R., Vanderschueren, D., Manolagas, S.C., 2017. Estrogens and androgens in skeletal physiology and pathophysiology. Physiol. Rev. 97, 135–187.
Callewaert, F., Venken, K., Ophoff, J., De Gendt, K., Torcasio, A., van Lenthe, G.H., Van Oosterwyck, H., Boonen, S., Bouillon, R., Verhoeven, G., et al., 2009. Differential regulation of bone and body composition in male mice with combined inactivation of androgen and estrogen receptor-alpha. FASEB J. 23, 232–240.
Coffey, K., Robson, C.N., 2012. Regulation of the androgen receptor by post-translational modifications. J. Endocrinol. 215, 221–237.
Dempster, D.W., Compston, J.E., Drezner, M.K., Glorieux, F.H., Kanis, J.A., Malluche, H., Meunier, P.J., Ott, S.M., Recker, R.R., Parfitt, A.M., 2013. Standardized nomenclature, symbols, and units for bone histomorphometry: a 2012 update of the report of the ASBMR Histomorphometry Nomenclature Committee. J. Bone Miner. Res. 28, 2–17.
Erben, R.G., Glosmann, M., 2012. Histomorphometry in rodents. Methods Mol. Biol. 816, 279–303.
Falahati-Nini, A., Riggs, B.L., Atkinson, E.J., O'Fallon, W.M., Eastell, R., Khosla, S., 2000. Relative contributions of testosterone and estrogen in regulating bone resorption and formation in normal elderly men. J. Clin. Invest. 106, 1553–1560.
Gareau, J.R., Lima, C.D., 2010. The SUMO pathway: emerging mechanisms that shape specificity, conjugation and recognition. Nat. Rev. Mol. Cell Biol. 11, 861–871.
Gustafsson, K.L., Farman, H., Henning, P., Lionikaite, V., Moverare-Skrtic, S., Wu, J., Ryberg, H., Koskela, A., Gustafsson, J.A., Tuukkanen, J., et al., 2016. The role of membrane ERalpha signaling in bone and other major estrogen responsive tissues. Sci. Rep. 6, 29473.
Kaikkonen, S., Jaaskelainen, T., Karvonen, U., Rytinki, M.M., Makkonen, H., Gioeli, D., Paschal, B.M., Palvimo, J.J., 2009. SUMO-specific protease 1 (SENP1) reverses the hormone-augmented SUMOylation of androgen receptor and modulates gene responses in prostate cancer cells. Mol. Endocrinol. 23, 292–307.
Kawano, H., Sato, T., Yamada, T., Matsumoto, T., Sekine, K., Watanabe, T., Nakamura, T., Fukuda, T., Yoshimura, K., Yoshizawa, T., et al., 2003. Suppressive function of androgen receptor in bone resorption. Proc. Natl. Acad. Sci. U. S. A 100, 9416–9421.
Khosla, S., Monroe, D.G., 2018. Regulation of bone metabolism by sex steroids. Cold Spring Harb. Perspect. Med. 8, a031211.
Leder, B.Z., LeBlanc, K.M., Schoenfeld, D.A., Eastell, R., Finkelstein, J.S., 2003. Differential effects of androgens and estrogens on bone turnover in normal men. J. Clin. Endocrinol. Metab. 88, 204–210.
Mellström, D., Vandenput, L., Mallmin, H., Holmberg, A.H., Lorentzon, M., Oden, A., Johansson, H., Orwoll, E.S., Labrie, F., Karlsson, M.K., et al., 2008. Older men with low serum estradiol and high serum SHBG have an increased risk of fractures. J. Bone Miner. Res. 23, 1552–1560.
Moverare-Skrtic, S., Henning, P., Liu, X., Nagano, K., Saito, H., Börjesson, A.E., Sjögren, K., Windahl, S.H., Farman, H., Kindlund, B., et al., 2014. Osteoblast-derived WNT16 represses osteoclastogenesis and prevents cortical bone fragility fractures. Nat. Med. 20, 1279–1288.
Nilsson, M.E., Vandenput, L., Tivesten, A., Norlen, A.K., Lagerquist, M.K., Windahl, S.H., Börjesson, A.E., Farman, H.H., Poutanen, M., Benrick, A., et al., 2015. Measurement of a comprehensive sex steroid profile in rodent serum by high-sensitive gas chromatography-tandem mass spectrometry. Endocrinology 156, 2492–2502.
Orwoll, E.S., 2001. Androgens: basic biology and clinical implication. Calcif Tissue Int 69, 185–188.
Poukka, H., Karvonen, U., Janne, O.A., Palvimo, J.J., 2000. Covalent modification of the androgen receptor by small ubiquitin-like modifier 1 (SUMO-1). Proc. Natl. Acad. Sci. U. S. A. 97, 14145–14150.
Sutinen, P., Malinen, M., Heikkinen, S., Palvimo, J.J., 2014. SUMOylation modulates the transcriptional activity of androgen receptor in a target gene and pathway selective manner. Nucleic Acids Res. 42, 8310–8319.
Vanderschueren, D., Laurent, M.R., Claessens, F., Gielen, E., Lagerquist, M.K., Vandenput, L., Börjesson, A.E., Ohlsson, C., 2014. Sex steroid actions in male bone. Endocr. Rev. 35, 906–960.
Vinel, A., Hay, E., Valera, M.C., Buscato, M., Adlanmerini, M., Guillaume, M., Cohen-Solal, M., Ohlsson, C., Lenfant, F., Arnal, J.F., et al., 2016. Role of ERalpha in the effect of estradiol on cancellous and cortical femoral bone in growing female mice. Endocrinology 157, 2533–2544.
Wilkinson, K.A., Henley, J.M., 2010. Mechanisms, regulation and consequences of protein SUMOylation. Biochem. J. 428, 133–145.
Wu, J., Moverare-Skrtic, S., Börjesson, A.E., Lagerquist, M.K., Sjögren, K., Windahl, S.H., Koskela, A., Grahnemo, L., Islander, U., Wilhelmson, A.S., et al., 2016. Enzalutamide reduces the bone mass in the axial but not the appendicular skeleton in male mice. Endocrinology 157, 969–977.
Wu, J., Movérare-Skrtic, S., Zhang, F.P., Poutanen, M., Ohlsson, C., 2016. Androgen receptor SUMOylation regulates bone mass in male mice. J. Bone Miner. Res. 31 (Suppl. 1) Available at: http://www.asbmr.org/education/AbstractDetail?aid=4282e188-9dca-4641-8731-ebfff811a962, Accessed date: 22 March 2018.